**The vibrational progression of the NV electronic transition of ethylene: a test case for the computation of Franck-Condon factors of highly flexible photoexcited molecules**

R. BORRELLI; PELUSO A. The vibrational progression of the NV electronic transition of ethylene: a test case for the computation of Franck-Condon factors of highly flexible photoexcited molecules. THE JOURNAL OF CHEMICAL PHYSICS. 125 pp: 194308-194316.
DOI: 10.1063/1.2388269

# The vibrational progressions of the $N \rightarrow V$ electronic transition of ethylene. A test case for the computation of Franck-Condon factors of highly flexible photoexcited molecules

Raffaele Borrelli and Andrea Peluso

October 11, 2006

**Abstract**

The vibrational progressions of the $N \rightarrow V$ electronic transition of ethylene - a test case for the computation of Franck-Condon factors between electronic states exhibiting very different equilibrium geometries - have been calculated by using both the Cartesian and the curvilinear internal coordinate representations of the normal modes of vibration. The comparison of the theoretical spectra with the experimental one shows that the Cartesian representation yields vibrational progressions which are not observed in the experimental spectrum, whereas the curvilinear one gives a very satisfying agreement, even in harmonic approximation.

# Introduction

Duschinsky's normal mode transformation is a fundamental tool for understanding mechanistic details of both radiative and radiationless photochemical processes in polyatomic molecules.[1] It relates the two sets of normal modes of vibration of two electronic states, a necessary step for the computation of the Franck-Condon factors, and provides valueable information about modes which change their equilibrium positions and modes which are mixed each other for the effect of the electronic transition. Displaced and, to a lesser extent, mixed modes determine the shape of the absorption bands and the dynamics of radiationless processes.

Duschinky's transformation turned out to work very well for transitions between electronic states characterized by small displacements of the nuclear equilibrium configurations. Much less is known about its application to transitions between electronic states whose equilibrium geometries are significantly different. Large displacements of the equilibrium geometries characterize many interesting photochemical processes, such as, among many others, the fast photoisomerization of retinal,[2,3] the unusual fast intersystem crossing of norbornene,[4,5] and, very probably, the fast internal conversion observed in some of DNA bases.[6]

The photophysical properties of these processes are obviously dominated by motion along the large amplitude vibrational coordinate and therefore simplified theoretical models, employing only the large amplitude coordinate and, in some cases, a few others, are often sufficient to explain the qualitative features of both the absorption spectrum and the interconversion dynamics.[7] However, when a better quantitative agreement between theoretical and experimental results is needed, the whole set of the molecular vibrational coordinates has to be taken into account, as for pyrazine $S_2 \rightarrow S_1$ internal conversion,[8] and Duschinsky's normal mode transformation become a necessary step for the evaluation of the Franck-Condon factors, and a powerful tool for understanding the dynamics of the electronic transition.[9]

Normal modes of vibration are the most natural set of vibrational coordinates to be used, since they form a complete and orthogonal set of coordinates for the internal motion of a molecule. Normal modes are usually expressed in terms of

mass weighted Cartesian displacement coordinates, but it is well known that in some cases it is more convenient to express them in terms of internal curvilinear coordinates such as bond distances, valence angles, torsions, waggings, etc.[10] For small amplitudes of vibration about the equilibrium point the two representations are practically identical, but for large amplitude motions they are not, because no single rectilinear coordinate can describe a large change of a valence or torsional angle without simultaneously introducing large change in one or more bond distances. Because of that, Duschinsky's normal mode transformation can give very different results in the two coordinate representations.[11,12]

In this paper we will more deeply analyze this point by performing a detailed comparison between experimental and theoretical spectra obtained by computations of the Franck-Condon (FC) factors both in the Cartesian and the internal coordinate representation. The vibrational progression patterns which characterize most of the gas-phase electronic spectra of molecules undergoing large geometry rearrangement at the excited state are the most suited experimental data for testing the accuracy of theoretical models in describing the vibrational motion in the region of the nuclear coordinates spanned by photoisomerization processes. Here we will consider the case of ethylene. The rotation about the carbon-carbon bond occurring in the $\pi \rightarrow \pi^*$ transition being a prototype of a large amplitude motion induced by a radiative transition, for which a well resolved absorption spectrum in the gas phase has been reported in the literature.[13–15] Previous theoretical works have not considered the whole set of normal modes,[7,16–18] but for a few of them all using the Cartesian representation.[19,20]

The UV spectrum of ethylene has a very complex structure, resulting from the overlap of several electronic transitions whose assignments are still subject of controversy. The electronic transitions are in fact relatively closely spaced and most of the involved excited states have equilibrium geometries significantly different from that of the ground state. In this paper we will only focus on the lowest energy $\pi \rightarrow \pi^*$ absorption, taking place between 48000 and 56000 $cm^{-1}$ (208-178 nm), which exhibits a vibrational progression with an extremely weak onset, almost unanimously[21]

attributed to the transition between the ground $^1A_{1g}$ electronic state (denoted as $N$) and the excited singlet $^1B_{1u}$ state ($V$).

# Normal Mode Transformation in Curvilinear and Cartesian coordinates

Let $\mathbf{Q}_1$ and $\mathbf{Q}_2$ be the normal mode vectors of a molecule in the electronic states $|1\rangle$ and $|2\rangle$, respectively. In the 30's Duschinsky suggested that the two sets of normal coordinates are related by the expression:[1]

$$\mathbf{Q}_1 = \mathbf{J}\mathbf{Q}_2 + \mathbf{K}, \tag{1}$$

where $\mathbf{J}$ is a rotation matrix and $\mathbf{K}$ a displacement vector, the former accounting for mixing of normal modes upon electronic transition, the latter for changes in the nuclear equilibrium configurations.

If $\mathbf{Q}_1$ and $\mathbf{Q}_2$ are expressed in terms of Cartesian coordinates $\boldsymbol{\xi}$,

$$\mathbf{Q}_\alpha = \mathbf{T}_\alpha^+ \mathbf{m}^{1/2}(\boldsymbol{\xi} - \boldsymbol{\xi}_\alpha^0) \qquad \alpha = 1, 2, \tag{2}$$

then:

$$\mathbf{J}^{(x)} = \mathbf{T}_1^+ \mathbf{m}^{-1} \mathbf{T}_2, \qquad \mathbf{K}^{(x)} = \mathbf{T}_1^+ \mathbf{m}^{-1/2}(\boldsymbol{\xi}_2^0 - \boldsymbol{\xi}_1^0), \tag{3}$$

where $\mathbf{m}$ is the diagonal matrix of the atomic masses, and $\mathbf{T}_\alpha$ and $\boldsymbol{\xi}_\alpha^\circ$ are the normal mode matrix and the equilibrium position vector of the electronic state $|\alpha\rangle$.

If normal modes are expressed in terms of a set of $3N-6$ non-redundant internal coordinates $\mathbf{s}$ ($N$ =number of atoms):

$$\mathbf{Q}_\alpha = \mathbf{L}_\alpha^{-1}(\mathbf{s} - \mathbf{s}_\alpha^0) \qquad \alpha = 1, 2, \tag{4}$$

then:

$$\mathbf{J}^{(s)} = \mathbf{L}_1^{-1} \mathbf{L}_2, \qquad \mathbf{K}^{(s)} = \mathbf{L}_1^{-1}(\mathbf{s}_2^0 - \mathbf{s}_1^0), \tag{5}$$

where $\mathbf{s}_\alpha^0$ is the vector of the equilibrium internal coordinates in the electronic state $|\alpha\rangle$, and $\mathbf{L}_\alpha$ is the normal mode matrix in internal coordinates. Of course, equation 5 holds only if the same set of non-redundant internal coordinates is used for both electronic states.

Most of the modern packages for electronic wave function computations give normal modes of vibration in the Cartesian representation. The normal mode matrix in internal coordinate representation ($\mathbf{L}_\alpha$) can then be obained from $\mathbf{T}_\alpha$ by expanding internal coordinates in power series of Cartesian coordinates around the equilibrium position and truncating the expansion at the first order:[10]

$$\mathbf{s} = \mathbf{s}^0_\alpha + \mathbf{B}_\alpha(\boldsymbol{\xi} - \boldsymbol{\xi}^0_\alpha), \quad \alpha = 1, 2 \tag{6}$$

where $\mathbf{B}_\alpha$ is the first derivative matrix, known as Wilson matrix.[22]

From the inverse transformation:

$$\boldsymbol{\xi} = \boldsymbol{\xi}^0_\alpha + \mathbf{G}^{-1}_\alpha \mathbf{B}^+_\alpha \mathbf{m}^{1/2}(\mathbf{s} - \mathbf{s}^0_\alpha), \tag{7}$$

with

$$\mathbf{G}_\alpha = \mathbf{B}^+_\alpha \mathbf{m}^{-1/2} \mathbf{B}_\alpha, \tag{8}$$

and using eq.s 2, and 5, the following relations for the transformation from $\mathbf{Q}_2$ to $\mathbf{Q}_1$, equivalent to those found by Reimers,,[12] are found:

$$\mathbf{J}^{(s)} = \mathbf{T}^+_1 \mathbf{m}^{-1/2} \mathbf{B}^+_1 \mathbf{G}^{-1}_1 \mathbf{B}_2 \mathbf{m}^{-1/2} \mathbf{T}_2, \tag{9}$$

$$\mathbf{K}^{(s)} = \mathbf{T}^+_1 \mathbf{m}^{-1/2} \mathbf{B}_1 \mathbf{G}^{-1}_1 (\mathbf{s}^0_1 - \mathbf{s}^0_2). \tag{10}$$

The matrices $\mathbf{J}^{(x)}$, $\mathbf{K}^{(x)}$ or $\mathbf{J}^{(s)}$, $\mathbf{K}^{(s)}$, together with the vibrational frequencies of the normal modes of the two electronic states provide all the necessary parameters to calculate FC integrals in the harmonic approximation. The evaluation of these integrals can be easily done by using recurrence relations.[23,24] In our calculation we have used the MolFC package, developed by our research group.[25]

In the case the two electronic states exhibit large equilibrium geometry differences, the normal mode transformation in the Cartesian representation can differ from eq. 1 because of the necessary fulfilling of the Eckart conditions in both electronic states (the so called axis switching effect).[26–28] By considering only static Eckart conditions, the correction term consists in applying a rotation matrix $\mathbf{T}_0$ to the normal mode matrix and to the equilibrium position vector of one electronic state. In the cartesian representation the Duschinsky matrix and the displacement vector take the form:

$$\mathbf{J}^{(x)} = \mathbf{T}_1^+ \mathbf{m}^{-1} \mathbf{T}_0 \mathbf{T}_2, \qquad \mathbf{K}^{(x)} = \mathbf{T}_1^+ \mathbf{m}^{-1/2} (\mathbf{T}_0 \boldsymbol{\xi}_2^0 - \boldsymbol{\xi}_1^0), \tag{11}$$

where:

$$\mathbf{T}_0 = (\mathbf{C}^+ \mathbf{C})^{1/2} \mathbf{C}^{-1}, \quad C_{ij} = \sum_k^N (\boldsymbol{\xi}_{1,k}^0)_i (\boldsymbol{\xi}_{2,k}^0)_j, \qquad i,j = x,y,z \tag{12}$$

A similar equation also holds for $\mathbf{J}^{(s)}$ and $\mathbf{K}^{(s)}$

In the case of ethylene, $\mathbf{T}_0$ is the identity matrix, since the principal axes of rotation of the two equilibrium nuclear configurations coincide.[28]

# The electronic spectrum of ethylene

In the ground electronic state ($N$), ethylene has a planar configuration with $D_{2h}$ symmetry. In the first excited electronic singlet state ($V$), the two methylenic groups are perpendicular each other and the molecule belongs to the $D_{2d}$ point group. Because of this large structural change, the absorption spectrum of ethylene exhibits an unusually broad vibrational progression, with the onset at 208 nm. The absorption intensity, initially vanishingly small, increases by about five order of magnitude before reaching the maximum at 1620 $\mathring{A}$. In this region the $N \rightarrow V$ transition overlaps with the first member of the strong Rydberg series found by Price and Tutte,[29] denoted by Mulliken as $N \rightarrow R$ transition. A quantitative analysis of the spectrum in this region goes beyond the scopes of this work; since we are interested in the vibrational pattern associated with the twisting motion, we will limit the analysis to the spectral region 208-178 nm, where only the $N \rightarrow V$ transition takes place.

The equilibrium geometry and the normal modes of vibrations of the ground electronic state have been obtained by *ab initio* calculation; the effects of the electronic correlation have been taken into account by using the second order Moeller-Plesset perturbation theory (MP2), $D_{2h}$ symmetry was imposed in geometry optimization. For the first excited state, geometry optimization and normal mode calculation have been carried out by using the singly excited configuration interaction (CIS) method, imposing $D_2$ symmetry. In both cases the standard 6-311++G(p,d) basis set has

been emploied. Following Wiberg *et al.*,[30] the calculated frequencies of the $V$ excited state have been scaled by the empirical value 0.9. All the electronic calculations were carried out by G94 package.[31] The optimized geometries and the frequencies of the normal modes of the $N$ and $V$ electronic states are reported in tables I and II, respectively.

INSERT TABLE I

INSERT TABLE II

**The Cartesian coordinate representation**. The rotation matrix $\mathbf{J}^{(x)}$ and the displacement vector $\mathbf{K}^{(x)}$ for the $N \rightarrow V$ normal mode transformation in the Cartesian representation are reported in table III.

INSERT TABLE III

Within the $D_2$ symmetry subgroup, common to both $N$ and $V$ electronic states, the normal modes of ethylene are grouped into four subsets, as indicated in table II. Inspection of table III shows that all the modes belonging to the same irreducible representation are strongly mixed, in particular the twisting of the $CH_2$ groups ($\nu_4$) and the symmetric combination of the four CH stretchings ($\nu_1$), belonging to the $a$ representation. The displacement vector $\mathbf{K}^{(x)}$ has four non zero components associated with the totally symmetric modes, whose numerical values agree perfectly with those previously reported.[32] The most displaced modes are the twisting and the symmetric CH stretching (7.18 and 4.15 in adimensional units, respectively); the symmetric scissoring ($\nu_3$) and the CC stretching ($\nu_2$) modes also exhibit large shifts of their equilibrium positions. It is worth noticing that the large $\mathbf{K}^{(x)}$ component of the $\nu_1$ mode is not due to changes of the C-H equilibrium bond lengths, which, according to *ab-initio* computations, are extremely small, *cf.* table 1, but rather to the mixing of the symmetric stretching vibration with the $CH_2$ twisting, which makes the large displacement of the latter mode to be partially projected on the former. This mixing occurs only in the Cartesian normal mode representation and disappears when internal coordinates are used, see *infra*.

The absorption spectrum, calculated exciting all the twelve normal modes of the $V$ state and letting the $N$ state be in its vibronic ground state, is shown in figure 1a. The convergence of the calculation with respect to the size of the adopted vibrational basis set has been accurately checked. The four displaced modes are of course the most important modes in the vibrational progression, but $b_3$ and $b_2$ modes contribute up to 30% to the overlap integral between the ground vibronic state of $N$ with the manifold of the $V$ vibronic states.

INSERT FIGURE 1

The computed spectrum is exceedingly broad, extending over more than 70000 $cm^{-1}$, whereas the experimental absorption band, including both the $N \rightarrow V$ and the $N \rightarrow R$ transitions, has a width no larger than 21000-22000 $cm^{-1}$. According to our calculation the 0-0 FC factor is vanishingly small, $10^{-14}$, and the maximum intensity, $3.5 \cdot 10^{-3}$ is associated with the transition from the ground vibronic state to the $4_0^{21}2_0^1 1_0^7$ combination state, located at 37000 $cm^{-1}$ above the 0-0 transition. (In the notation adopted here a vibronic transition is denoted by $X_i^j$, where $X$ labels the normal mode, *cf.* table II, and $i$ and $j$ the vibrational quantum numbers of the ground and excited state, respectively.)

The computed and the observed absorption intesities[33] in the region 49000-56000 $cm^{-1}$ are reported in figure 2a. In order to have the best intensity matching, the peak at 49140 $cm^{-1}$ (2035 $\AA$) has to be assigned to the $4_0^5$ transition. Although figure 2a shows a reasonable agreement between theoretical and experimental intensities, it must be remarked that the above assignment is not only in significant disagreement with previous work of Wilkinson and Mulliken, who assigned this peak to the $4_0^{11}$ transition, but it also leads to large discrepancies between the calculated and the observed spectrum at higher transition energies. In fact, the maximum absorption is predicted at about 85000 $cm^{-1}$ (*ca.* 1170 $\AA$), *cf.* figure 1a, whereas the N→V transition ends at 70420 $cm^{-1}$ (*ca.* 1420 $\AA$).

INSERT FIGURE 2

A quantitative comparison between the computed and the experimental spectrum in the region of the maximum absorption is not possible because of the overlapping $N \rightarrow R$ transition; however the large broadness which characterizes the theoretical spectrum is clearly in disagreement with the experimental data. In harmonic approximation that discrepancy arises from the large shift of the symmetric C-H stretching mode. Indeed, if excitations of this mode are not considered in the calculation of the FC factors, the vibrational progression of the theoretical absorption spectrum becomes sharper and less intense, as shown in figure 1b. In that case the maximum of the absorption band is predicted to fall at about 60000 $cm^{-1}$ (1666 $\mathring{A}$), and the whole theoretical spectrum ends at 70000 $cm^{-1}$ (1428 $\mathring{A}$), in reasonable agreement with the experimental one.

In conclusion, the main features of the experimental spectrum are better reproduced, in harmonic approximation, by neglecting excitations of the CH stretching mode. The strong involvement of this mode predicted by Duschinsky transformation of the normal modes in Cartesian representation has not any experimental counterpart, resonance Raman spectra do not show any activity associated with this vibration.[34]

**The internal coordinate representation**. The whole set of CH and CC stretchings, the four $\angle$CCH bendings, the two out of plane $\angle CCH_2$ bendings, and the torsion angle between the planes of the two $CH_2$ groups constitute the set of internal non-redundant coordinate adopted here. The last coordinate is defined, following reference 35, as a linear combination of the four HCCH dihedrals. The elements of the rotation matrix $\mathbf{J}^{(s)}$ and of the displacement vector $\mathbf{K}^{(s)}$ are reported in table IV

Insert Table IV

In the internal coordinate representation, the $CH_2$ twisting mode is no longer coupled to any of the other totally symmetric normal coordinates; that makes the CH symmetric stretching component of $\mathbf{K}^{(s)}$ vanishingly small, *cf.* table IV, as it would be expected from *ab-initio* computations. The CC stretching and the $CH_2$ scissoring modes also exhibit much smaller equilibrium displacements.

The theoretical spectrum calculated by exciting all the twelve normal modes is reported in figure 1c.

The computed spectrum shows a well defined vibrational structure arising from excitations of the $CH_2$ twisting and the $CH_2$ scissoring modes, no progression associated with the symmetric CH stretching mode is predicted. The most intense vibrational progression is of course associated with the twisting vibration; the other two progressions, clearly visible in figure 1c, are due to combination bands of the type $4_0^n 3_0^1$ and $4_0^n 3_0^2$, in order of decreasing intensity. The highest FC factor is 0.055 for the $4_0^{25}$ transition, more than one order of magnitude higher than that obtained employing the Cartesian coordinate representation; the overall band width is about 20000 $cm^{-1}$.

The best matching between the computed and the observed intensities is obtained by assigning the peak at 49140 $cm^{-1}$ to the $4_0^7$ transition, see figure 2b. With this assignment the 0-0 transition falls at 43140 $cm^{-1}$, and the calculated maximum absorption peak, corresponding to the $4_0^{25}$ transition, is located at about 63000 $cm^{-1}$ (1587 Å). Both the region of the maximum absorption as well as the whole spectral width are in good qualitative agreement with the experimental data. The agreement on peak intensities is good up to 52000 $cm^{-1}$; slight discrepancies are observed at higher wavenumbers, but, in this case, they could be due to the neglect of anharmonic effects. Indeed, in this spectral region the energies of the vibronic states populated by the radiative $N \rightarrow V$ transition are well above the barrier associated to the rotation about the CC bond; the wavefunction for twisting no longer behaves as a harmonic oscillator, or even as a perturbed harmonic oscillator, but it better resembles that of a free rotator.[36]

**The internal rotator model**. Taking advantage of the separability of the $a$ modes in the curvilinear representation, *cf.* table IV, the torsional internal coordinate can be treated indipendently from all the others as a hindered rotator in a potential field of the form:[37,38]

$$V^{(N)} = \sum_{k=1}^{3} \frac{V_k^{(N)}}{2} \left[1 + \cos\left(2k\tau\right)\right], \tag{13}$$

for the $N$ state, and

$$V^{(V)} = \sum_{k=1}^{3} \frac{V_k^{(V)}}{2} \left\{ 1 + \cos\left[ 2k \left( \tau + \frac{\pi}{2} \right) \right] \right\}, \tag{14}$$

for the $V$ state.

The coefficients of $V^{(N)}$ were obtained by Wallace from fitting of experimental data,[39] the numerical values are ($\mathrm{cm}^{-1}$): $V_1^{(N)} = 20454$, $V_2^{(N)} = -2040$, $V_3^{(N)} = 295$. For the $V$ state, the Siebrand recipe $V_k^{(V)} = 0.73 V_k^{(N)}$ has been adopted.[7] This choice yields an energy barrier for rotation about the CC bond slightly larger than that obtained by *ab-initio* multiconfigurational methods,[40] 19920 *vs.* 17200 $\mathrm{cm}^{-1}$. However Siebrand's potential has been used succesfully for the analysis of the ethylene spectrum and therefore we have preferred to adopt it, even for allowing an easier comparison between the present results and those already reported in the literature.

The Hamiltonian operator for the torsional motion is:[41]

$$\left[ -B^{(\alpha)} \frac{\partial^2}{\partial^2 \tau} + V^{(\alpha)} \right] |\tau_n(\alpha)\rangle = E_n \, |\tau_n(\alpha)\rangle \qquad \alpha = N, V \tag{15}$$

where $B^{(\alpha)} = \hbar^2 / I_{CH_2}^{(\alpha)}$, and $I_{CH_2}^{(\alpha)}$ is the moment of inertia of the methylenic group about the axis passing through the two carbon atoms in the electronic state $|\alpha\rangle$.

From the calculated equilibrium geometries, *cf.* table I, $B_{CH_2}^{(N)} = 19.503$ $\mathrm{cm}^{-1}$, and $B_{CH_2}^{(V)} = 20.455$ $\mathrm{cm}^{-1}$ .

By expanding the eigenstates $\left|\tau_n^{(\alpha)}\right\rangle$ in a finite Fourier series,

$$\left|\tau_n^{(\alpha)}\right\rangle = \frac{1}{\sqrt{2\pi}} \sum_{k=-M}^{M} c_{nk} e^{ik\tau} \qquad \alpha = N, V, \tag{16}$$

the energies and the wavefunctions of the quantum states associated with the twisting motion can be easily found by diagonalizing the Hamiltonian matrices of the $N$ and $V$ electronic states.

A good convergence on the energies of the quantum states of interest for the $N \rightarrow V$ transition has been found by using 250 exponential functions for both the $N$ and $V$ states. Franck-Condon factors have been then computed as the product of

two terms, one for the twisting coordinate, the other for all the remaining normal modes:

$$\mathrm{FC}_{N\to V} = |\langle\tau_n(N)|\tau_m(V)\rangle\langle\mathbf{Q}_N|\mathbf{Q}_V\rangle|^2. \tag{17}$$

In that way Duschinky effect due to normal mode mixing is fully accounted for.

In figure 1d the absorption spectrum obtained from the internal rotator model is shown. The agreement between computed and observed peak intensities and wavenumbers is almost quantitative up to 54000 $\mathrm{cm}^{-1}$. As in the case of the harmonic approximation, the most intense vibrational progression is associated with excitations of the twisting mode alone, and the two lower intensity progressions are due to combination bands of the type $4_0^n 2_0^1$ and $4_0^n 2_0^2$, respectively. The highest Franck-Condon integral (*ca.* 0.17) is associated with the $4_0^{20}$ transition. The absorption intensity decays quite quickly, in about 7000 $\mathrm{cm}^{-1}$ from the maximum intensity peak. The overall bandwidth is *ca.* 10000 $\mathrm{cm}^{-1}$, much less than that obtained in the harmonic approximation. This result rules out the possibility that the continuum background observed at shorter wavelengths can be attributed to the $N \to V$ transition.

The best matching between observed and calculated intensities is obtained by assigning the peak at 49140 to the $4_0^9$ transition, see figure 2c, in quite good agreement with Mulliken's assignment. With this choice the 0-0 transition falls at 42325$\mathrm{cm}^{-1}$ , and the most intense vibronic transitions occur at 56683 and 57182 $\mathrm{cm}^{-1}$. No peaks are observed at these wavenumbers, but, as first suggested by Mulliken,[15] they are probably hidden by the beginning of the $N \to R$ transition.

# Conclusions

From the results discussed above several important points emerge.

First of all, in harmonic approximation the two coordinate representations give very different results; the broad and structureless spectrum calculated by using the Cartesian representation of normal modes becomes a sharper and more intense band when the computation of the FC integrals is carried out in internal coordinates. The broadness of the theoretical spectrum obtained by using the Cartesian representa-

tion is mainly caused by the large equilibrium displacement of the symmetric CH stretching normal mode upon electronic transition. This large displacement has no experimental counterpart: no vibrational progression has been assigned in the past to this mode and, furthermore, resonance Raman spectra have not shown any significant activity of this mode in the $N \rightarrow V$ transition.[34] *Ab-initio* computations are in line with the above experimental findings, the equilibrium CH bond lengths of the $N$ and $V$ states are predicted to differ by only 0.005 Å. Although the CH activity has been invoked to explain the continuum background appearing in the ethylene spectrum below 1600 Å,[20,32] exactly in that region of shorter wavelengths the computed spectrum strongly disagrees with the observed one.

The shapes of the theoretical spectra obtained in the internal coordinate representation agree with the experimental data, as well as with that obtained by a different approach, in which the absorption profile is obtained as the Fourier transform of the autocorrelation function.[42] In the case of the hindered rotator model the agreement with the observed spectrum is almost quantitative in the wavelength region where only the $N \rightarrow V$ transition takes place, but even the harmonic model turns out to be sufficient for a qualitative assignment of the observed spectral peaks. According to our results, the peak at 49140 has to be to assigned to the $4_0^9$ transition in the internal rotator model and to the $4_0^7$ one in harmonic approximation. The latter value has to be taken as a lower limit; the assignment of this peak to lower vibrational excited states, as occurs in the Cartesian representation, leads to theoretical spectra which are significantly broader than the observed one. The fact that the internal rotator model does not show any absorption continuum associated with the $N \rightarrow V$ transition is not a serious drawback, because other mechanisms can account for it; non-adiabatic couplings between closely lying electronic excited states has been often invoked, even though the nature of the coupled states is still a matter of debate.[40,43]

As concerns the application of Duschinsky's normal mode transformation to cases where the equilibrium geometries of the two electronic states are significantly different, the results presented here clearly show that Duschinsky's transformation works

well when the normal modes are expressed in terms of a non-redundant set of internal curvilinear coordinates. In the Cartesian representation, a large equilibrium displacement of one coordinate can be partially projected on some of the others, giving rise to the appearance in the computed electronic spectrum of vibrational progressions which are not experimentally observed. Mostly important, in the internal coordinate representation normal mode mixing occurs to a much lesser extent than in the Cartesian coordinate representation. This offers several advantages both in the treatment of anharmonic effects and in dynamic computations, where normal mode separability plays a crucial role.[44]

The work presented here is only the first necessary step toward a quantitative simulation of the ethylene absorption spectrum. Non adiabatic coupling as well as the variation of the transition moment with the torsional angle[38,42] play certainly a role; work is in progress along these lines.

# Acknowledgments

The financial support of the University of Salerno and of the MIUR is gratefully acknowledged.

# References and Notes


1. Duschinsky, F. *Acta Phisicochim. URSS* **1937,** *7,* 551-566.

2. Schoenlein, R. W.; Peteanu, L.; Mathies, R.; Shank, C. *Science* **1991,** *254,* 412.

3. Wang, Q.; Schoenlein, R. W.; Peteanu, L. A.; Mathies, R. A.; Shank, C. *Science* **1994,** *266,* 422.

4. Grimme, S.; Woeller, M.; Peyerimhoff, S. D.; Dannovich, D.; Shaik, S. *Chem. Phys. Lett.* **1998,** *287,* 601.

5. Barwise, A. J. G.; Gorman, A. A.; Rodgers, M. A. J. *Chem. Phys. Lett.* **1976,** *38,* 313.

6. Crespo-Hernández, C. E.; Cohen, B.; Hare, P. M.; Bern, K. *Chem. Rev.* **2004,** *104,* 1977–2020.

7. Siebrand, W.; Zerbetto, F.; Zgrieski, M. Z. *Chem. Phys. Lett.* **1990,** *174,* 119-125.

8. Raab, A.; Worth, G. A.; Meyer, H.-D.; Cederbaum, L. S. *J. Chem. Phys.* **1999,** *110,* 936.

9. Borrelli, R.; Peluso, A. *J. Chem. Phys.* **2003,** *119,* 8437–8448.

10. Wilson, E. B. J.; Decius, J. C.; Cross, P. C. *Molecular vibrations;* Dover Publications, New York: 1980.

11. Sibert, E. L. I.; Hynes, J. T.; Reinhardt, W. P. *J. Phys. Chem.* **1983,** *87,* 2032-2037.

12. Reimers, J. R. *J. Chem. Phys.* **2001,** *115,* 9103-9109.

13. Zelikoff, M.; Watanabe, K. *J. Opt. Soc. Am.* **1953,** *43,* 756-759.

14. Schmitt, R. G.; Brehm, R. K. *App. Opt.* **1966,** *5,* 1111-1116.

15. Wilkinson, P. G.; Mulliken, R. S. *J. Chem. Phys.* **1955,** *23,* 1895-1907.

16. Petrongolo, C.; Buenker, R. J.; Peyerrimhoff, S. D. *J. Chem. Phys.* **1983,** *78,* 7284.

17. Hazra, A.; Chanh, H. H.; Nooijen, M. *J. Chem. Phys.* **2004,** *121,* 2125-2136.

18. Siebrand, W.; Zerbetto, F.; Zgrieski, M. Z. *J. Chem. Phys.* **1989,** *91,* 5926-5933.

19. Mebel, A. M.; Chen, Y.-T.; Lin, S.-H. *J. Chem. Phys.* **1996,** *105,* 9007-9020.

20. Mebel, A. M.; Hayashi, M.; Liang, K. K.; Lin, S. H. *J. Phys. Chem. A* **1999,** *103,* 10674-10690.

21. Snyder, P. A.; Sylvia, A.; Hansen, R. W. C. *J. Phys. Chem. A* **2004,** *108,* 4194-4201.

22. Califano, S. *Vibrational States;* John Wiley and Sons Ltd: 1976.

23. Doktorov, E. V.; Malkin, I. A.; Manko, V. I. *J. Mol. Spec.* **1975,** *56,* 1-20.

24. Peluso, A.; Santoro, F.; Del Re, G. *Int. J. Quant. Chem.* **1997,** *63,* 233-244.

25. Borrelli, R.; Peluso, A. "MolFC: A program for Franck-Condon integrals calculation", Package available free of charge via Internet at `http://www.theochem.unisa.it`.

26. Houghen, J. T.; Watson, J. K. G. *Can. J. Phys.* **1965,** *43,* 298.

27. Lucas, N. J. D. *J. Phys. B: Atom. Molec. Phys.* **1973,** *6,* 155.

28. Özkan, I. *J. Mol. Spec.* **1990,** *139,* 147.

29. Price, W. C.; Tutte, W. T. *Proc. Roy. Soc. London A* **1940,** *174,* 207–220.

30. Wiberg, K. B.; Hadad, C. M.; Foresman, J. B.; Chupka, W. A. *J. Phys. Chem.* **1992,** *96,* 10756-10768.

31. Frisch, M. J.; Trucks, G. W.; Schlegel, H. B.; Gill, P. W.; Johnson, B. G.; Robb, M. A.; Cheeseman, J. R.; Keith, T.; Petersson, G. A.; Montgomery, J. A.; Raghavachari, K.; Al-Laham, M. A.; Zakrzewski, V. G.; Ortiz, J. V.; Foresman, J. B.; J., C.; B., S. B.; Nanayakkara, A.; Challacombe, M.; Peng, C. Y.; Ayala, P. Y.; Chen, W.; Wong, M. W.; Andres, J. L.; Repogle, E. S.; Gomperts, R.; Martin, R. L.; Fox, D. J.; Binkley, J. S.; Defrees, D. J.; Baker, J.; Stewart, J. P.; Head-Gordon, M.; Gonzales, C.; Pople, J. A. *Gaussian 94, Revision C.2;* Gaussian Inc.: Piittsburgh PA: 1995.

32. Mebel, A. M.; Chen, Y.-T. C.; Lin, S.-H. *Chem. Phys. Lett.* **1996,** *258,* 53-62.

33. McDiarmid, R. *J. Chem. Phys.* **1967,** *47,* 1517-1524.

34. Sension, R. J.; Hudson, B. S. *J. Chem. Phys.* **1989,** *90,* 1337-1389.

35. Miyazawa, T.; Fukushima, K. *J. Mol. Spec.* **1965,** *15,* 308-318.

36. Peyerimoff, S. D.; Buenker, R. J. *Theoret. Chim. Acta* **1972,** *27,* 243-264.

37. Watson, J. K. G.; Siebrand, W.; Pawlikowski, M.; Zgierski, M. Z. *J. Chem. Phys.* **1996,** *105,* 1348-1354.

38. Merer, A. J.; Watson, James, K. G. *J. Mol. Spec.* **1973,** *47,* 499-514.

39. Wallace, R. *Chem. Phys. Lett.* **1989,** *159,* 35-36.

40. Krawkczyk, R. P.; Viel, A.; Manthe, U.; Domcke, W. *J. Chem. Phys.* **2003,** *119,* 1397-1411.

41. Wallace, R.; Leroy, J. P. *Chem. Phys.* **1990,** *144,* 371-376.

42. Ben-Nun, M.; Martínez, T. J. *J. Phys. Chem. A* **1999,** *103,* 10517-10527.

43. Ben-Nun, M.; Martínez, T. J. *Chem. Phys.* **2000,** *259,* 237-248.

44. Borrelli, R.; Di Donato, M.; Peluso, A. *Biophys. J.* **2005,** *89,* 830-841 in press.

45. Mulliken, R. S. *J. Chem. Phys.* **1955,** *23,* 1997-2011.

**Figure captions**

**Figure 1**. Theoretical spectra of ethylene obtained by different methods: a) using the Cartesian coordinate representation of normal coordinates and excitations on all the twelve modes; b) as (a) but with no excitation of the CH stretching mode; c) using the internal coordinate representation and excitations on all modes; d) treating the torsional motion as an internal hindered rotation and all the other normal modes in the internal curvilinear representation.

**Figure 2**. Computed (sticks) and observed (•) vibrational progressions of the $N \rightarrow V$ transition. a) Cartesian coordinate representation, Cost=9.0.; b) internal coordinate representation, Cost = 6.1; c) internal rotator model, Cost= 5.2. Observed intensities from ref. 33.

Table I: Optimized molecular geometry parameters for the ground and the first excited singlet state of ethylene.

| | Electronic state | |
|---|---|---|
| | $N$ | $V$ |
| CC | 1.339 | 1.373 |
| CH | 1.085 | 1.090 |
| ∠HCH | 117.19 | 112.91 |
| ∠HCCH | 0° | 88.48° |

Table II: Computed vibrational frequencies ($cm^{-1}$) of the $N$ and $V$ states of ethylene. The frequencies of the $V$ state have been scaled by 0.9.

| Notation[a] | Description | $D_{2h}$ | $D_2$ | $N$ | $V$ |
|---|---|---|---|---|---|
| $\nu_1$ | CH stretch. | $a_g$ | $a$ | 3192.8 | 2820.0 |
| $\nu_2$ | CC stretch | $a_g$ | $a$ | 1674.9 | 1220.4 |
| $\nu_3$ | $CH_2$ sciss. | $a_g$ | $a$ | 1382.1 | 1376.4 |
| $\nu_4$ | torsion | $a_u$ | $a$ | 1057.9 | 851.1 |
| $\nu_5$ | CH stretch. | $b_{1u}$ | $b_1$ | 3175.2 | 2783.6 |
| $\nu_6$ | $CH_2$ sciss. | $b_{1u}$ | $b_1$ | 1481.6 | 1246.3 |
| $\nu_7$ | $CH_2$ wag | $b_{2g}$ | $b_2$ | 756.0 | 909.0 |
| $\nu_8$ | CH stretch | $b_{2u}$ | $b_2$ | 3291.6 | 2836.4 |
| $\nu_9$ | $CH_2$ rock | $b_{2u}$ | $b_2$ | 829.5 | 659.6 |
| $\nu_{10}$ | CH stretch | $b_{3g}$ | $b_3$ | 3264.9 | 2835.9 |
| $\nu_{11}$ | $CH_2$ rock | $b_{3g}$ | $b_3$ | 1237.5 | 903.2 |
| $\nu_{12}$ | $CH_2$ wag | $b_{3u}$ | $b_3$ | 956.7 | 670.2 |

a) Reference 45

Table III: Duschinsky matrix $\mathbf{J}^{(x)}$ and adimensional normal mode displacements $\mathbf{K}^{(x)}$ in the Cartesian coordinate representation.

| | $\mathbf{J}^{(x)}$ | | | | | | | | | | | | $\mathbf{K}^{(x)}$ |
|---|---|---|---|---|---|---|---|---|---|---|---|---|---|
| Mode | $\nu_1$ | $\nu_2$ | $\nu_3$ | $\nu_4$ | $\nu_5$ | $\nu_6$ | $\nu_7$ | $\nu_8$ | $\nu_9$ | $\nu_{10}$ | $\nu_{11}$ | $\nu_{12}$ | |
| $\nu_1$ | −0.80 | −0.14 | 0.01 | −0.58 | | | | | | | | | 4.17 |
| $\nu_2$ | −0.08 | −0.89 | −0.31 | 0.33 | | | | | | | | | −1.50 |
| $\nu_3$ | −0.11 | −0.24 | 0.94 | 0.22 | | | | | | | | | −1.98 |
| $\nu_4$ | 0.58 | −0.37 | 0.14 | −0.71 | | | | | | | | | 7.13 |
| $\nu_5$ | | | | | 0.79 | 0.14 | | | | | | | |
| $\nu_6$ | | | | | 0.11 | 0.92 | | | | | | | |
| $\nu_7$ | | | | | | | −0.75 | −0.58 | 0.33 | | | | |
| $\nu_8$ | | | | | | | −0.41 | 0.78 | 0.45 | | | | |
| $\nu_9$ | | | | | | | 0.49 | −0.17 | 0.82 | | | | |
| $\nu_{10}$ | | | | | | | | | | −0.80 | −0.27 | 0.53 | |
| $\nu_{11}$ | | | | | | | | | | 0.14 | −0.95 | −0.26 | |
| $\nu_{12}$ | | | | | | | | | | 0.58 | −0.13 | 0.80 | |

Table IV: Duschinsky matrix $\mathbf{J}^{(s)}$ and adimensional normal mode displacemets $\mathbf{K}^{(s)}$ in the internal coordinate representation.

| | $\mathbf{J}^{(s)}$ | | | | | | | | | | | | $\mathbf{K}^{(s)}$ |
|---|---|---|---|---|---|---|---|---|---|---|---|---|---|
| | $\nu_1$ | $\nu_2$ | $\nu_3$ | $\nu_4$ | $\nu_5$ | $\nu_6$ | $\nu_7$ | $\nu_8$ | $\nu_9$ | $\nu_{10}$ | $\nu_{11}$ | $\nu_{12}$ | |
| $\nu_1$ | −1.00 | −0.05 | −0.02 | 0.00 | | | | | | | | | −0.04 |
| $\nu_2$ | 0.04 | −0.95 | −0.29 | 0.02 | | | | | | | | | 0.14 |
| $\nu_3$ | 0.00 | −0.29 | 0.96 | 0.00 | | | | | | | | | −0.89 |
| $\nu_4$ | 0.00 | −0.02 | −0.01 | −1.02 | | | | | | | | | 8.07 |
| $\nu_5$ | | | | | 1.00 | 0.05 | | | | | | | |
| $\nu_6$ | | | | | −0.05 | 0.99 | | | | | | | |
| $\nu_7$ | | | | | | | 0.67 | −0.06 | −0.57 | | | | |
| $\nu_8$ | | | | | | | 0.00 | 1.00 | 0.02 | | | | |
| $\nu_9$ | | | | | | | 0.55 | 0.09 | 1.01 | | | | |
| $\nu_{10}$ | | | | | | | | | | −1.00 | 0.00 | −0.02 | |
| $\nu_{11}$ | | | | | | | | | | 0.09 | −0.79 | −0.43 | |
| $\nu_{12}$ | | | | | | | | | | −0.06 | −0.66 | 0.77 | |

Figure 1

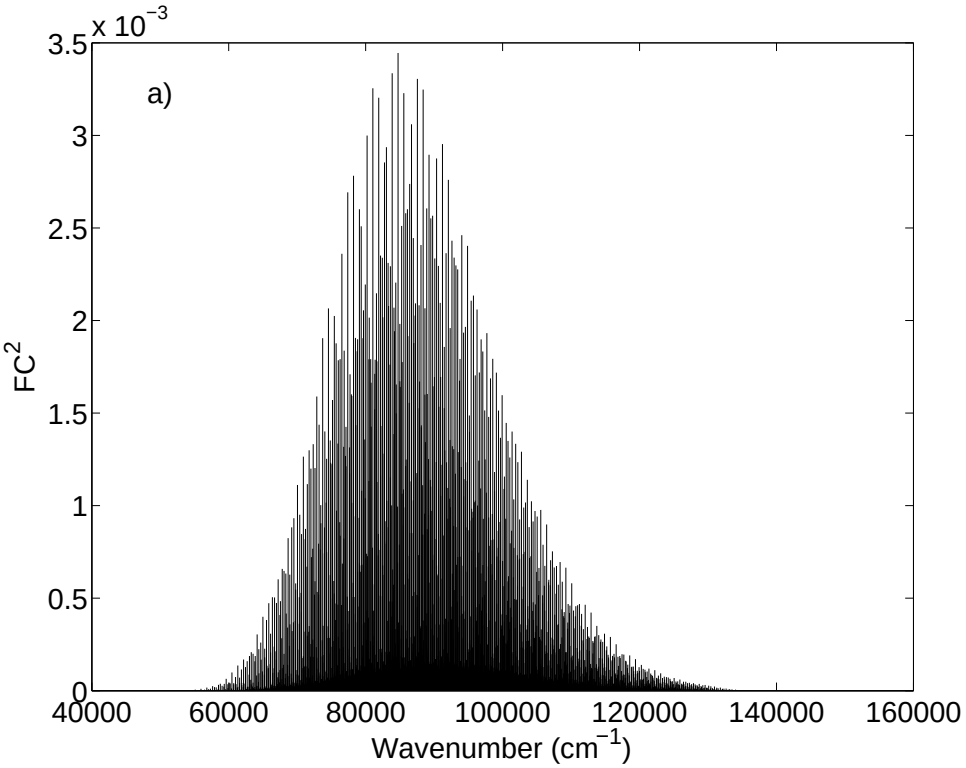


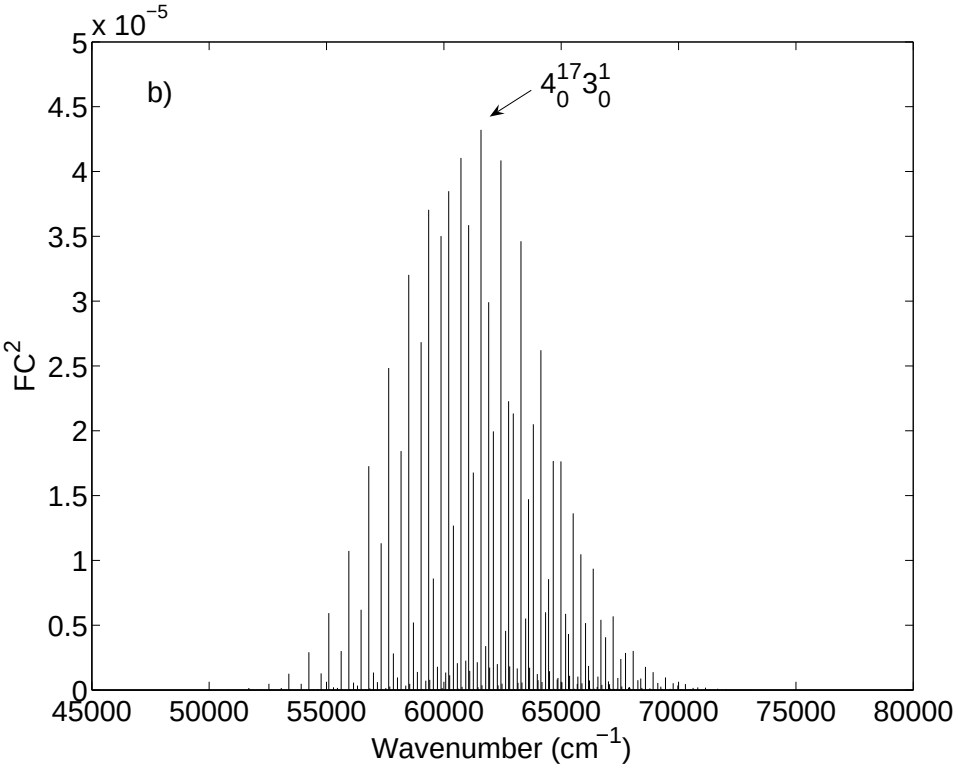

Figure 1

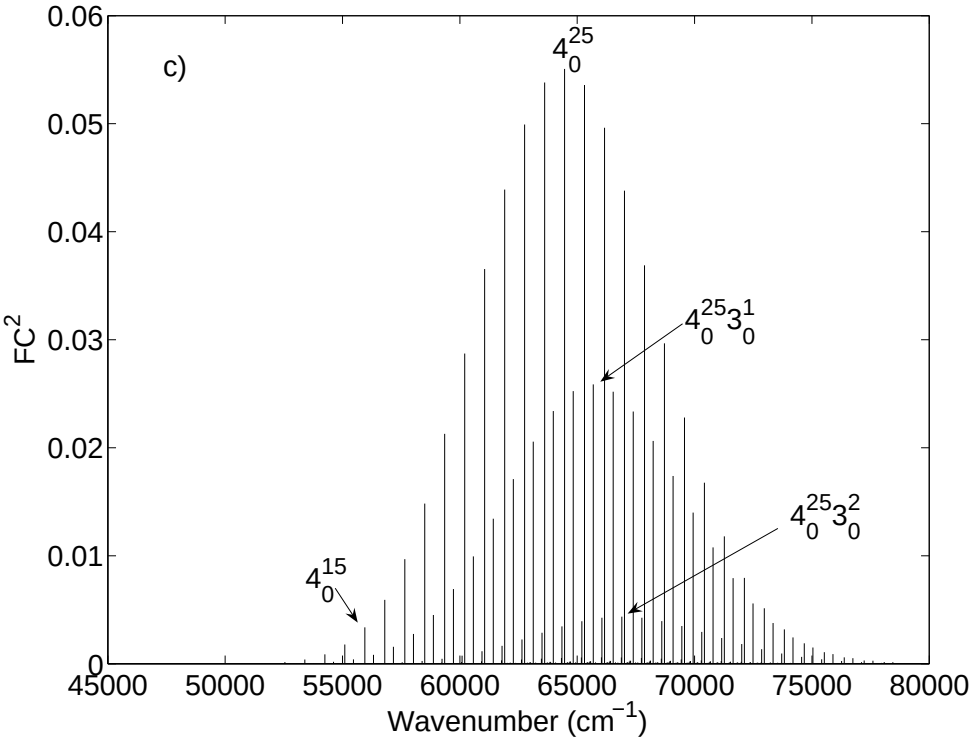
c)
$4_0^{25}$
$4_0^{25}3_0^1$
$4_0^{25}3_0^2$
$4_0^{15}$
FC$^2$
Wavenumber (cm$^{-1}$)
0
0.01
0.02
0.03
0.04
0.05
0.06
45000
50000
55000
60000
65000
70000
75000
80000

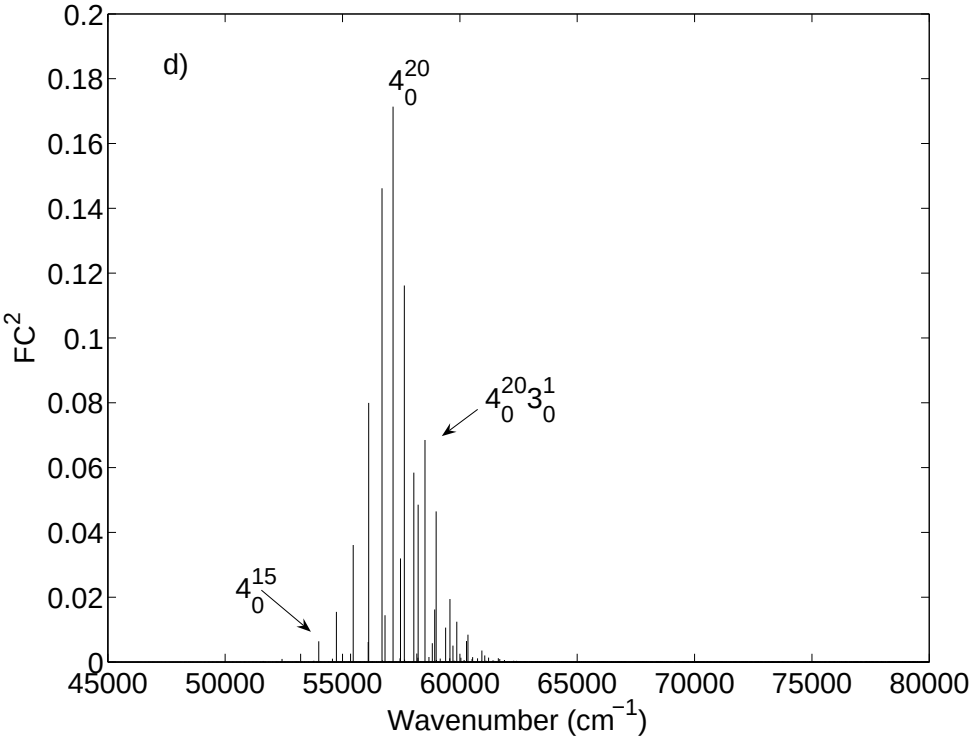
d)
$4_0^{20}$
$4_0^{20}3_0^1$
$4_0^{15}$
FC$^2$
Wavenumber (cm$^{-1}$)
0
0.02
0.04
0.06
0.08
0.1
0.12
0.14
0.16
0.18
0.2
45000
50000
55000
60000
65000
70000
75000
80000

Figure 2

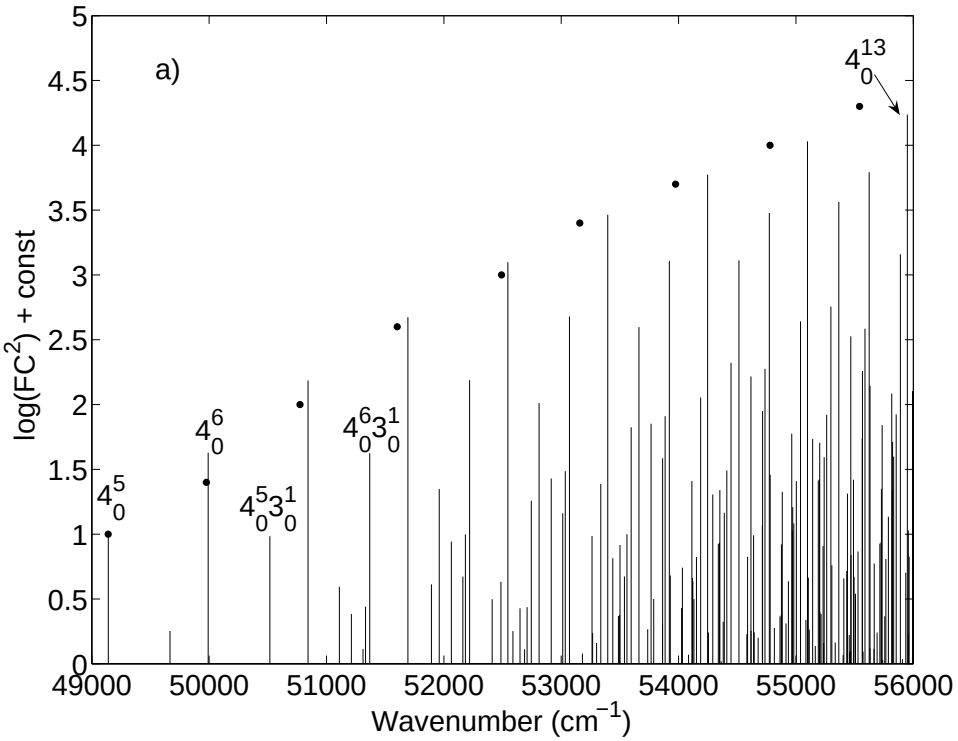
a)
$4_0^{13}$
$4_0^6$
$4_0^6 3_0^1$
$4_0^5$
$4_0^5 3_0^1$
log(FC$^2$) + const
Wavenumber (cm$^{-1}$)

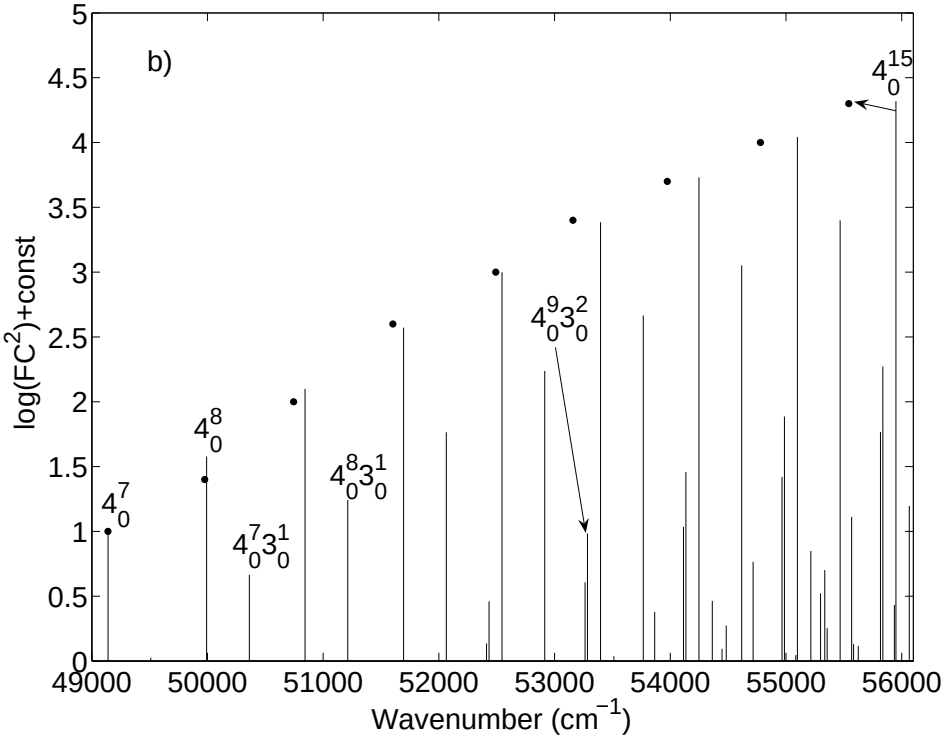
b)
$4_0^{15}$
$4_0^9 3_0^2$
$4_0^8$
$4_0^8 3_0^1$
$4_0^7$
$4_0^7 3_0^1$
log(FC$^2$)+const
Wavenumber (cm$^{-1}$)

Figure 2

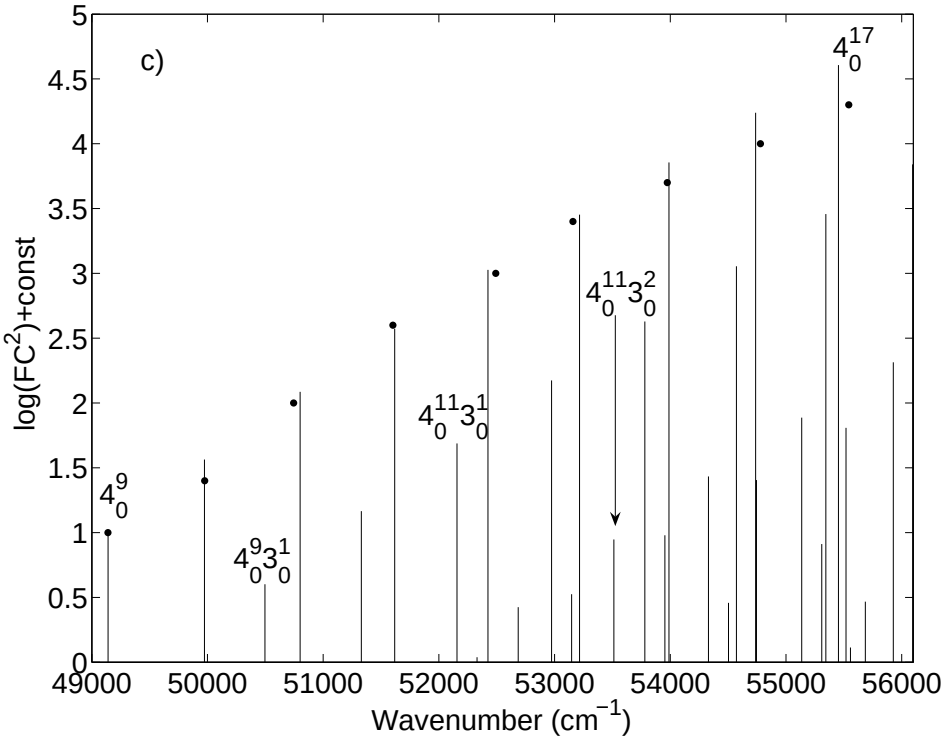
c)
$4_0^{17}$
$4_0^{11}3_0^2$
$4_0^{11}3_0^1$
$4_0^9$
$4_0^9 3_0^1$
log(FC$^2$)+const
Wavenumber (cm$^{-1}$)
0
0.5
1
1.5
2
2.5
3
3.5
4
4.5
5
49000
50000
51000
52000
53000
54000
55000
56000